# Anisotropic irreversibility of the Abrikosov and Josephson flux dynamics in $YBa_{2-x}Sr_xCu_3O_{7-\delta}$ single crystals: Bose-glass and vortex-glass features

V. N. Vieira and J. Schaf*
*Instituto de Física, Universidade Federal do Rio Grande do Sul - UFRGS, CEP 91501-970, Porto Alegre-RS, Brazil*
(Received 26 November 2001; published 5 April 2002)

Very detailed magnetic irreversibility data for fields applied along the $c$ axis or the $ab$ plane of a pure and untwinned $YBa_2Cu_3O_{7-\delta}$ single crystal and Sr-doped and heavily twinned $YBa_{2-x}Sr_xCu_3O_{7-\delta}$ ($x=0.25$, 0.37, and 0.5) single crystals are reported. The irreversibility lines $T_{irr}(H)$ of the pure single crystal show a considerable planar anisotropy but follow the same power-law regime, for both field orientations, arising within the conventional flux-creep theories in the whole field range. Very differently, however, the $T_{irr}(H)$ lines of the doped superconductors exhibit besides large anisotropies, several different regimes. In fields lower than 8 kOe the $T_{irr}(H)$ data of the doped samples display the de Almeida–Thouless (AT) and Gabay-Toulouse (GT)-like power-law behaviors, the signature of a frustrated superconductor. For higher-field values, and in particular for $H\|c$, flux dynamics seems to be conventional. However, for $H\|ab$ and field values above 30 kOe, the flux dynamics displays sharp directional properties along the twinning planes (TP's) for rotations about the $c$ axis. This behavior is cusplike, comparable to that caused by columnar defects, which characterizes a Bose-flux-glass phase. We appoint the superconducting granularity and frustration as responsible for the AT and GT behaviors below 8 kOe and the strong anisotropic pinning for $H$ parallel to the TP's as the cause of the Bose-glass features. On the other hand, the isotropic pinning for large angular displacements or for any angle in fields below 30 kOe is the most probable cause of the vortex-glass features.

DOI: 10.1103/PhysRevB.65.144531 PACS number(s): 74.25.Ha, 74.62.Dh, 74.72.Bk, 74.80.Bj

## I. INTRODUCTION

The magnetic irreversibility in type-II superconductors arises from the viscous flow of the magnetic flux under a driving force, assisted by thermal activation and opposed by pinning forces from defects and surface barriers. This magnetic irreversibility persists up to a certain temperature limit $T_{irr}$ ($T_{irr}<T_c$) that varies with the applied field, and depends on the nature of the pinning physics of the superconductor. The form of the irreversibility line is thus pervaded with information about the pinning mechanisms. High-$T_c$ oxide superconductors (HTSC's), prepared without special care, are normally granular and not homogeneous superconductors. Their magnetic behavior thus depends on two different kinds of flux dynamics; that of the intergrain Josephson flux and that of the intragrain Abrikosov flux. In order to reach the grains in the bulk or release them, the magnetic flux has to traverse the intergrain spaces. Hence flux blockage at the intergrain spaces acts cumulatively on that within the grains. Nevertheless the flux stabilizing mechanisms of each kind of flux has its own peculiarities. The extraordinary complexity of the flux dynamics in the HTSC's comes mainly from the entanglement of these two kinds of mechanisms.

Many irreversibility studies[1–9] of HTSC's as a function of applied field, especially on very clean single crystals, revealed a surprisingly simple power-law behavior that relates the irreversibility field to the irreversibility temperature $T_{irr}(H)$:

$$H_{irr}(T)=H_0^{fc}(1-t^{fc})^{\alpha} \quad (\alpha=\tfrac{3}{2}). \tag{1}$$

Here $t^{fc}=T_{irr}^{fc}(H)/T_{irr}^{fc}(0)$ and $H_0^{fc}$ as well as $T_{irr}^{fc}(0)$ are fitting parameters. This power law arises within the conventional flux-creep (fc) theory[10] under the regime of giant flux creep.[1] The basic assumption underlying this theory is that the superconductor is homogeneous, which is accomplished in conventional superconducting metals as well as in nearly perfect high-$T_c$ single crystals. This, however, is in clear conflict with the observed two-step resistive transition, observed in all imperfect HTSC's, which denotes granularity.[11–15] While the higher-temperature step marks the pairing transition within the grains, the second step is related to the coherence transition of the grain aggregate. Although the behavior of the magnetic irreversibility line of granular HTSC's conforms to Eq. (1) in a vast high-field region, where the intragranular Abrikosov-flux dynamics dominates, it systematically falls off this regime in a low-field region. The nice description of the magnetic state of the conventional superconductors in terms of an Abrikosov vortex lattice also becomes troubled in the granular superconductors. HTSC's have plenty of randomly located microscopic and mesoscopic lattice defects that act as isolated (isotropic) and/or correlated (anisotropic) pinning centers. In general the density and randomness of these pinning centers deform the flux line lattice so much that the concept of a lattice becomes inappropriate. When the temperature falls low enough, the vortex system freezes into a two-dimensional amorphous state, a vortex-glass phase. The existence of vortex-glass properties in HTSC's was theoretically predicted[16] (also see Refs. 17–20), and experimentally found in YBaCuO single crystals.[21]

For years YBaCuO single crystals and thin films having aligned columnar defects, caused by heavy-ion irradiation, have been known to exhibit strong pinning effects along the ion tracks.[22,23] Such cusplike directional effects were seen as Bose-glass properties. In recent years Bose-glass properties

 ©2002 The American Physical Society

of heavily twinned $YBa_2Cu_3O_{7-\delta}$ thick films[24] as well as large monodomain $YBa_2Cu_3O_{7-\delta}$ melt-textured samples[25] were also reported, and attributed to the correlated pinning of the twinning planes (TP's). The intersection of TP's with the intrinsic pinning planes constitutes a source of strongly directional pinning whose effects are in many respects analogous to that of the columnar defects. Several experimental techniques showed the role of TP's in flux dynamics as well as their effect on resistivity,[26] magnetization,[27] and critical current density.[28] No note, however, was made about Bose-glass properties in typical twinned single crystals.

Partial substitution (1 at.%) of Ba by Sr in the precursor oxides and carbonates of YBaCuO was found by electron microscopy[29] to result in substitutional Sr impurities at the Ba site. But this doping also gives rise to a high density of very tiny Sr precipitates within the crystal lattice. These Sr clusters are surrounded by strain fields that act as strong isotropic pinning centers. Besides the induction of a large peak effect in the magnetization cycles and correspondingly a hugely (up to 50 times) increased critical current, Sr doping also considerably reduces the magnetic irreversibility temperature limit $[T_{irr}(H)]$. This reduction was attributed[29] to a decoration of the twin planes by strain fields from nearby Sr clusters, but it may also be remarked that Sr doping depresses the critical pairing temperature $T_c$ that also reduces the irreversibility temperature. On the other hand, the fluctuation conductivity of YBaCuO, having 25% of Ba substituted for by Sr, revealed, besides a strong depression of $T_c$, an important reduction of the coherence length of the Ginsburg-Landau (GL) order parameter.[30] This sharpens even more the already steep topology of the GL order parameter reinforcing the superconducting granularity. An increase of granularity reflects itself in the resistive transition as a relative growth of the step corresponding to the coherence transition. But it also leads to a decrease in the overall slope of the magnetic irreversibility line.[12,30]

Recently we studied the $T_{irr}(H)$ of Sr-doped and heavily twinned $YBa_{2-x}Sr_xCu_3O_{7-\delta}$ single crystals ($x=0.25$ and 0.5) as well as of a polycrystalline sample for fields applied along the $c$ axis ($H\|c$).[30–33] The $T_{irr}(H)$ data of all these superconductors revealed a fc power law behavior [Eq. (1)] in a major high-field region. Nevertheless below 8 kOe the $T_{irr}(H)$ data gave account of two different regimes. In the lowest fields they follow a de Almeida–Thouless (AT)-like power law.[34]

$$H(T)=H_0^{AT}(1-t^{AT})^{\alpha} \quad \left(\alpha=\frac{3}{2}\right) \tag{2}$$

where $t^{AT}=T_{irr}^{AT}(H)/T_{irr}^{AT}(0)$, and $H_0^{AT}$ and $T_{irr}^{AT}(0)$ are fitting parameters. At about 0.8 kOe the $T_{irr}(H)$ data suddenly change slope and bend in the opposite sense, following a Gabay-Toulouse (GT)-like power law[35]

$$H=H_0^{GT}(1-t^{GT})^{\alpha} \quad \left(\alpha=\frac{1}{2}\right) \tag{3}$$

where $t^{GT}=T_{irr}^{GT}(H)/T_{irr}^{GT}(0)$, $H_0^{GT}$ and $T_{irr}^{GT}(0)$ are fitting parameters. If the behavior of the $T_{irr}(H)$ data for $(H\|c)$ is so rich, an obvious question concerns its behavior when $H$ points along the $ab$ plane.

The magnetic irreversibility limit of single-crystal HTSC's was found to be systematically higher for fields applied along the $ab$ plane ($H\|ab$) than for a field along the $c$ axis ($H\|c$).[5–9] These anisotropic $T_{irr}(H)$ data are usually ascribed to the intrinsic planar structure of the HTSC, and can be well fitted by Eq. (1) for both field directions. It should nevertheless be noted that the experimental data of practically all these irreversibility studies are much too discrete to reveal the finer details of the irreversibility line.

In the present work we extend our previous magnetic irreversibility $[T_{irr}(H)]$ study for fields along the $c$ axis[33] to the case of fields applied along the $ab$ planes ($H\|ab$). Besides large planar anisotropies and the same AT and GT power-law behaviors in low fields as for $H\|c$, we identify Bose-glass and vortex-glass features in high fields. We relate these properties to the anisotropic pinning of the twinning planes.

## II. SAMPLE PROCESSING AND MEASURING TECHNIQUES

The pure $YBa_2Cu_3O_{7-\delta}$ and the doped $YBa_{2-x}Sr_xCu_3O_{7-\delta}$ ($x=0.1$, 0.25, 0.37, and 0.5) single crystals were grown by the CuO flux method. The highly pure $Y_2O_3$, $BaCO_3$, $SrCO_3$ and CuO powders, thoroughly mixed in proportions $1:2(2-x):2x:10$ of Y, Ba, Sr, and Cu, respectively, were piled up on the higher side of a tilted (15°) $ZrO_2$ tray, and slowly heated in air from room temperature to 1020 °C for 10 h. The temperature was maintained at 1020 °C for 1 h and then uniformly cooled to 900 °C for 48 h. During this temperature ramp the saturated flux flows out from the mixture down to the lower side of the tray, and, on slowly evaporating, the single crystals grow out from the flux. Subsequently the furnace was cooled slowly past 700 °C and then down to room temperature. The single crystals in the form of thin platelets of about 0.1 mm in thickness are easily removed, as they stick little to the surface of the flux, attached to it only along the border. One crucial condition to be met, in order to succeed in growing crystals, is not heating the flux directly from above. In a second round the single crystals were encapsulated within two polycrystalline YBaCuO minidishes, and treated in pure flowing oxygen at 450 °C for ten days and then slowly cooled to room temperature. X-ray diffraction on several single crystals revealed no trace of strange phases, and the lattice parameters were in reasonable agreement with the values in the literature for the nominal Sr concentrations.[36–38] The superconducting transition temperatures $T_c$ were determined from the first inflection of the magnetization as a function of temperature, measured in fields of 10 Oe while slowly warming after zero-field cooling. Figure 1 displays the normalized magnetization curves for the different Sr concentrations. The $T_c$ values correspond to those in the literature,[36–38] and scale linearly with the Sr concentration.

An examination of single crystals with polarized light mi-

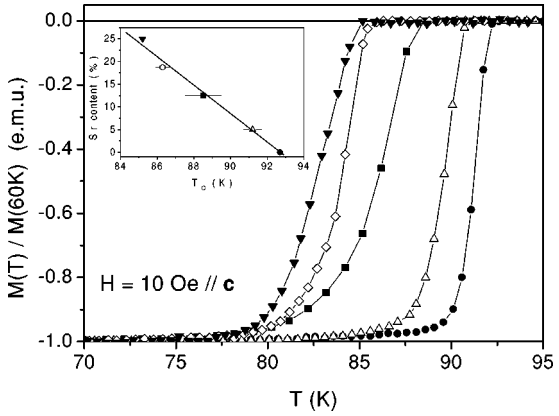


FIG. 1. The normalized $M(T)$ curves for $YBa_{2-x}Sr_xCu_3O_{7-\delta}$ ($x=0$, 0.1, 0.25, 0.37, and 0.5) samples. The inset displays $T_c$ as a function of the Sr concentration.

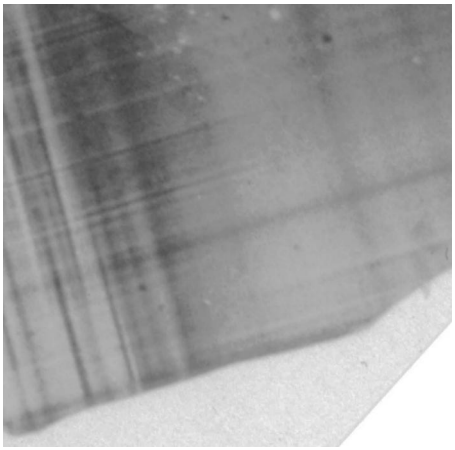

FIG. 2. Typical polarized light photoprint of a $YBa_{1.75}Sr_{0.25}Cu_3O_{7-\delta}$ single crystal for incidence along the $c$ axis and the analyzer at minimum transmission of reflected light.

croscopy, although unable to visualize individual twinning planes, shows the twin directions and the domain landscape of twinned regions. Most of our single crystals were heavily twinned, presenting mosaics of numerous small orthogonal twining domains similar to the findings by transmission electron microscopy.[29] Some were of monodomain nature, or showed several large twinning domains; others showed untwinned regions or were not twinned at all. Figure 2 exemplifies the kind of polarized light images for incidence along the $c$ axis and the analyzer turned to minimum transmission of the reflected light.

For our magnetic and magnetoresistivity measurements we chose heavily twinned single crystals that otherwise show a very clean appearance. The shape was approximately that of rectangles with somewhat irregular borders; see the sample dimensions in Table I. The plane of the single crystals could be aligned along the field direction to within 1° of precision. This alignment, although somewhat critical for low fields, becomes much more smooth for high fields.

The main experimental tool to investigate the magnetic irreversibility of superconductors is dc magnetization. For our magnetization measurements we used a SQUID (superconducting quantum interference device) MPMS-XL magnetometer from Quantum Design, and our method consisted of first cooling down the sample to temperatures well below $T_c$ in zero field [zero-field cooling (ZFC)]. Then, measuring the magnetization ($M_{ZFC}$) while slowly warming the sample ($0.2\ K/\mathrm{min}$ or less) up to $T \gg T_c$ in a constant field selected within 0.003-50 kOe, and subsequently measuring $M_{FC}$ while cooling back [field cooling (FC)] in the same field. Although this method is the most appropriate one for measurements of the magnetic irreversibilities, it can be significantly affected by residual temperature gradients because of its intrinsic temperature cycling. In the case of superconduct-

TABLE I. The fitting parameters of the single crystals $\alpha$, $H_0$, and $T_{irr}(0)$ for the various regimes, as found for each sample and for $H$ applied parallel to the $c$ axis or the $ab$ plane, are indicated by fc for the high-field flux-creep regime and by AT and GT for the two low-field frustration-dominated regimes.

| Samples (dimension) | fit | $H\|c$ $\alpha$ | $H_0$(kOe) | $T_{irr}(0)$(K) | $H\|ab$ $\alpha$ | $H_0$(kOe) | $T_{irr}(0)$(K) |
|---|---|---|---|---|---|---|---|
| $YBa_2Cu_3O_{7-\delta}$ $0.1\times0.2\times0.3$ mm$^3$ | fc | $1.50\pm0.05$ | 820.50 | 92.70 | $1.60\pm0.04$ | 4401.82 | 92.48 |
| $YBa_{1.75}Sr_{0.25}Cu_3O_{7-\delta}$-S1 | fc | $1.50\pm0.09$ | 475.91 | 89.04 | $1.53\pm0.15$ | 5210.52 | 87.72 |
| $0.1\times0.2\times0.3$ mm$^3$ | GT | $0.52\pm0.05$ | 25.57 | 87.15 | $0.48\pm0.06$ | 37.48 | 86.93 |
| | AT | $1.52\pm0.11$ | 661.31 | 87.88 | $1.52\pm0.12$ | 191.3 | 87.8 |
| $YBa_{1.75}Sr_{0.25}Cu_3O_{7-\delta}$-S2 | fc | $1.5\pm0.09$ | 464.16 | 89.46 | $1.6\pm0.2$ | 4163.56 | 87.7 |
| $0.1\times0.2\times0.3$ mm$^3$ | GT | $0.52\pm0.05$ | 25.57 | 87.15 | $0.55\pm0.1$ | 54.61 | 86.53 |
| | AT | $1.52\pm0.1$ | 661.31 | 87.88 | $1.52\pm0.15$ | 303.44 | 87.71 |
| $YBa_{1.63}Sr_{0.37}Cu_3O_{7-\delta}$ | fc | $1.4\pm0.09$ | 495.63 | 86 | $1.65\pm0.24$ | 5291.71 | 85.96 |
| $0.1\times0.2\times0.3$ mm$^3$ | GT | $0.60\pm0.07$ | 27.31 | 85.51 | $0.45\pm0.11$ | 18.68 | 85.44 |
| | AT | $1.45\pm0.38$ | 538.78 | 85.88 | $1.60\pm0.24$ | 1113.89 | 85.96 |
| $YBa_{1.5}Sr_{0.5}Cu_3O_{7-\delta}$ | fc | $1.50\pm0.08$ | 583.70 | 85.40 | $1.48\pm0.2$ | 2419.4 | 85 |
| $0.1\times0.2\times0.3$ mm$^3$ | GT | $0.50\pm0.05$ | 20.00 | 84.30 | $0.55\pm0.27$ | 41.94 | 83.64 |
| | AT | $1.51\pm0.05$ | 465.70 | 85.20 | $1.48\pm0.05$ | 379.5 | 85 |

ors these temperature gradients are also modulated by the variable thermal conductivity of these materials near $T_c$. Moreover, the low signal at the zero cross point near the superconducting transition, where the paramagnetic signal takes over the diamagnetic one, causes difficulties to the automatic sample centering system and thereby introducing distortions of the data about this region. All these effects are very misleading if not adequately bypassed. We first minimized the temperature gradients (to less than 0.1 K), and then corrected for the constant and linear terms in the residual temperature gradient and used a zero suppression technique to prevent the magnetic signal from crossing zero.

We also made magnetoresistivity measurements in order to obtain better insight into the superconducting granularity of our samples. To perform these measurements we used a four-contact technique in a low-current low-frequency ac experimental setup, where a lock-in amplifier was used as a null detector. During the measurements the temperature was swept very slowly (0.05 K/min) and measured with a Pt resistor corrected for magnetoresistance effects within a resolution of $2\times10^{-3}$ K. The magnetoresistance data points of the sample were closely spaced so that the temperature derivative of the resistivity, $d\rho/dT$ could be numerically calculated.

## III. EXPERIMENTAL RESULTS

### A. Magnetoconductivity

The resistive transition $\rho(T)$ of a granular superconductor occurs visibly in two stages, the temperature derivative ($d\rho/dT$) showing a well-defined peak related to the pairing transition and a shoulder at the lower-temperature side related to the coherence transition.[39] Even small applied fields are well known to distort the phase of the GL order parameter significantly within the grain junctions, thereby weakening their coupling energy and the pinning strength.[40] Magnetoresistivity measurements provide detailed information about the superconducting transition within the grains, the coherence transition, and the fluctuation conductivity.

In order to compare the resistive transitions of superconductors with different granularities, in Fig. 3 we display the magnetoresistive transitions and the respective temperature derivatives of our nearly perfect $YBa_2Cu_3O_{7-\delta}$ single crystal as well as of the doped $YBa_{1.9}Sr_{0.1}Cu_3O_{7-\delta}$ and $YBa_{1.75}Sr_{0.25}Cu_3O_{7-\delta}$ single crystals. The measurements were accomplished with low-density measuring currents and fields from zero to 0.6 kOe applied along the $ab$ plane. Note that, while the upper temperature peak of $d\rho/dT$ barely changes with an applied field, the shoulder or lower-temperature peak is strongly affected by it, becoming round and drastically decreased. This behavior of the shoulder characterizes it as a granularity effect related to the coherence transition. The complete absence of the shoulder in $d\rho/dT$ of the pure single crystal shows that this superconductor has a vanishing granularity and no junctions at all. The narrow and small secondary peaks at the lower-temperature side to the main peak of $d\rho/dT$ of the doped single crystal with $x=0.1$ shows that this sample has few superconducting grains linked by junctions of approximately the same quality. The analogous behavior of the lower-temperature peak of the single crystal with $x=0.25$ shows that this granular superconductor has many similar links.

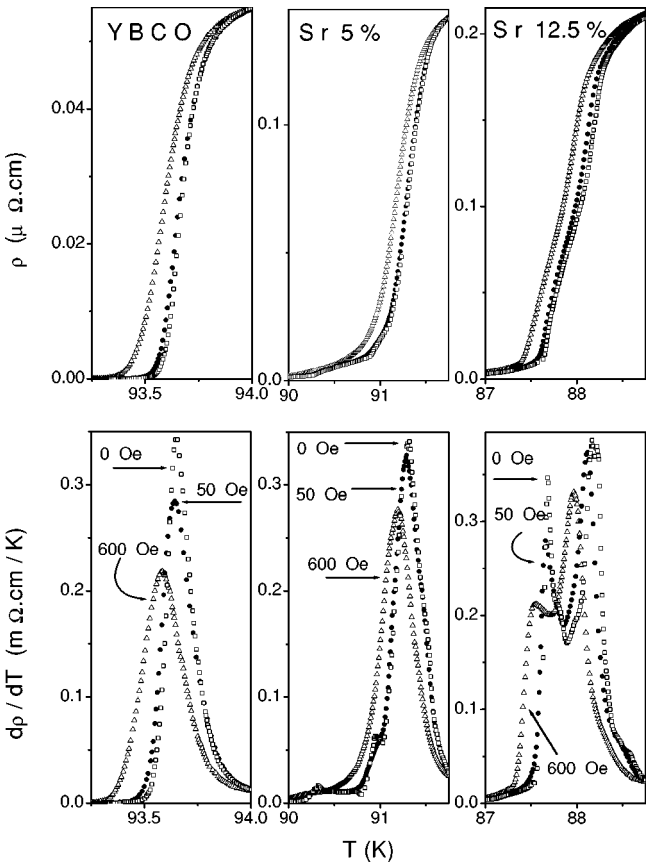


FIG. 3. The resistive transitions (upper panels) and the respective temperature derivates (lower panels) of the pure (left) and two doped (right) YBaCuO single crystals with the indicated Sr concentrations. The mesurements are for $H\|J\|ab$. We call attention to the different temperature scales and the drastic effect of the applied field on the coherence transition peak at the left-hand side of the main peak of the two doped samples.

### B. Magnetic irreversibilities

The magnetization along the $ab$ plane of our pure and doped YBaCuO single crystals is typically about an order of magnitude smaller than along the $c$ axis, but still within a range of very good resolution of the SQUID magnetometer. The ratio between the critical currents within the $CuO_2$ planes or normal to them is of about the same order. The most accurate determination of the magnetic irreversibility limit can be achieved by dc magnetization methods. We measured the magnetization while slowly warming the samples after zero-field cooling ($M_{ZFC}$), and subsequently $M_{FC}$, while cooling back in the same field. This was repeated for a large number of applied field values. Subtracting $M_{ZFC}$ from $M_{FC}$ for the same field value generates an array of difference data ($\Delta M = M_{FC}$-$M_{ZFC}$). The temperature point where the $\Delta M$ data abandon the zero base line, defined by the upper reversible temperature region, is the irreversibility limit ($T_{irr}$) for that field. While in high fields ($H>10$ kOe) $T_{irr}$ could be determined to within 0.5 K or better, in the lowest

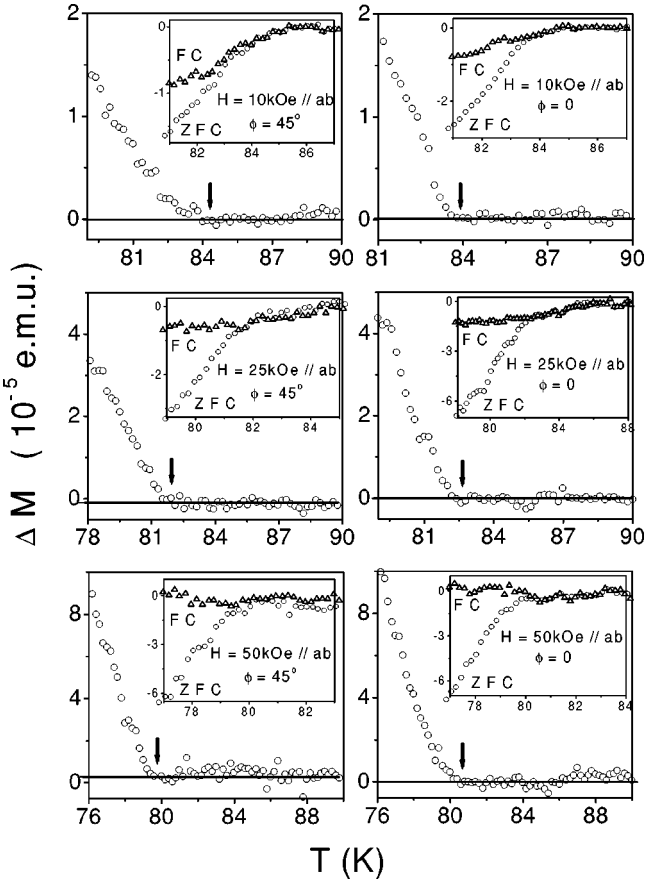


FIG. 4. Difference data $\Delta M = M_{FC} - M_{ZFC}$ of the $YBa_{1.63}Sr_{0.37}Cu_3O_{7-\delta}$ single crystal for the indicated field values ($H \| ab$). The three panels at the left display the data for a field at 45°, with respect to the TP's, and the right-hand panels that for fields parallel to the TP's. The vertical arrows indicate the irreversibility limit. The insets display the respective $M_{ZFC}$ and $M_{FC}$ data curves.

fields this precision improves to 0.2 K or better. On the other hand, the applied field could be read to within a fraction of an oersted after correcting for the remanent field of the superconducting coil.

An overview of our data analysis is displayed in Fig. 4, where examples of $\Delta M$ data are shown. There the vertical arrows indicate the irreversibility limits. The insets show the corresponding $M_{ZFC}$ and $M_{FC}$ data, which in general converge only asymptotically. Therefore, locating the irreversibility limit directly from the splitting of the $M_{ZFC}$ and $M_{FC}$ data is liable to considerable systematic error. The methods employed by some authors, using a minimum difference standard to delimit reversible from irreversible regimes, are very misleading since the convergence of $M_{ZFC}$ and $M_{FC}$ varies enormously with the applied field. The irreversibility limit can in general be located much more sharply in plots of the difference data $\Delta M$.

Plotting the $T_{irr}(H)$ data of a sample for the whole array of field values in a $H$-$T$ diagram defines its irreversibility line. Figure 5 displays the $T_{irr}(H)$ data of a pure $YBa_2Cu_3O_{7-\delta}$ single crystal for fields applied along the $ab$ plane ($H \| ab$) together with those for $H \| c$ from Ref. 33. The

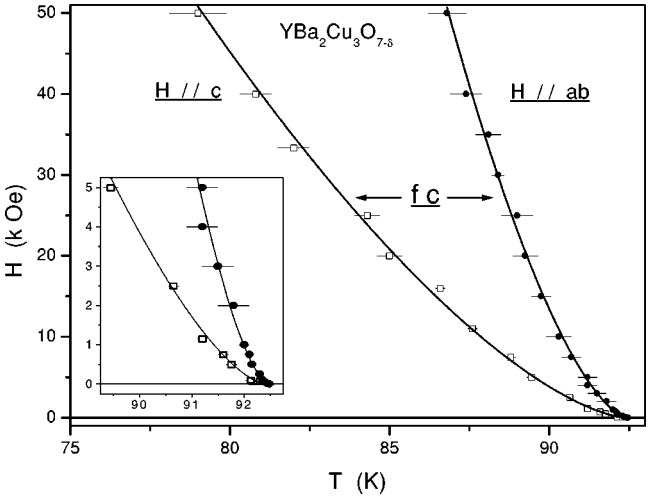


FIG. 5. The irreversibility data of the pure single crystal for $H \| c$ (left) and $H \| ab$ (right). The continuous curves are fittings to the fc power law from the flux-creep theories, [Eq. (1)]. We remark that the fitting is good in the whole field range.

continuous lines through these data are fittings to the fc power law [Eq. (1)]. The inset highlights the low-field details, and shows that the same fitting, good in the high-field range, also fits the low-field data well. The fitting parameters are given in Table I. The considerably anisotropic behavior of $T_{irr}(H)$ for $H \| c$ and $H \| ab$ is well known to be intrinsic to the planar superconducting structure of the HTSC. The $H$-$T$ diagrams for $T_{irr}(H)$ of the Sr-doped $YBa_{2-x}Sr_xCu_3O_{7-\delta}$ ($x = 0.25$ and 0.5) single crystals for $H \| ab$, are shown respectively in Figs. 6 and 7, together with

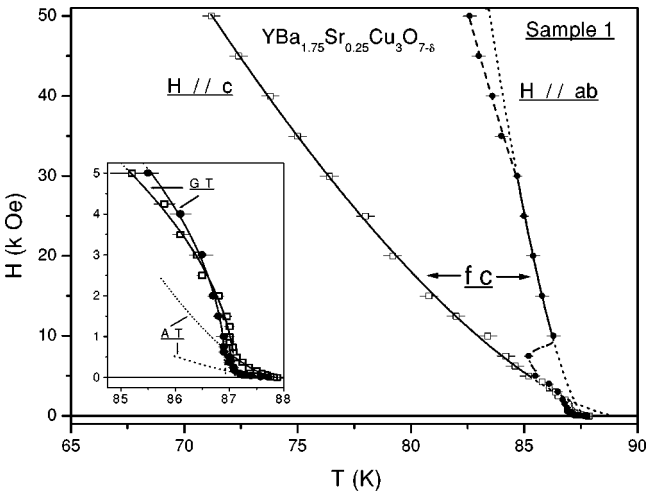


FIG. 6. The irreversibility data of the $YBa_{1.75}Sr_{0.25}Cu_3O_{7-\delta}$ single crystal (sample 1) for $H \| c$ (left) and $H \| ab$ (right). The continuous lines through these data are fittings to the fc power law. We remark that, for $H \| ab$, the data above a kink at about 30 kOe, fall increasingly to the left of the fitting, and in the low-field region fall systematically off the fittings for $H \| c$ as well as for $H \| ab$. The dashed line is a guide to the eye. The inset highlights the data in the low-field region. The continuous lines in the inset, indicated by AT or GT, are fittings to Eqs. (2) and (3), respectively. There is a sudden increase of the pinning at about 8 kOe for $H \| ab$.

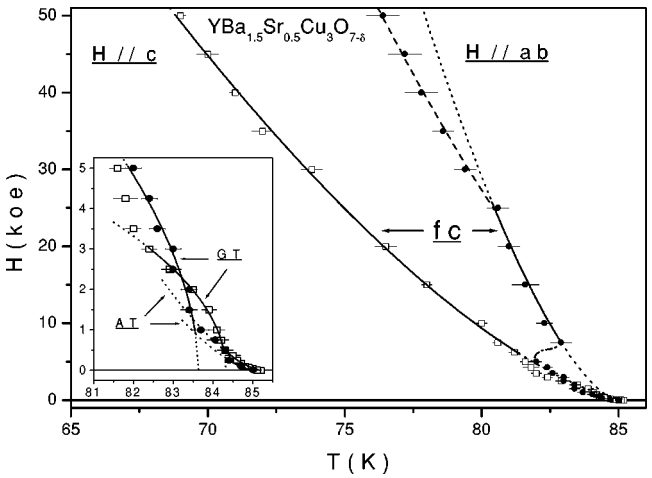


FIG. 7. Same as Fig. 6, but for sample $YBa_{1.5}Sr_{0.5}Cu_3O_{7-\delta}$.

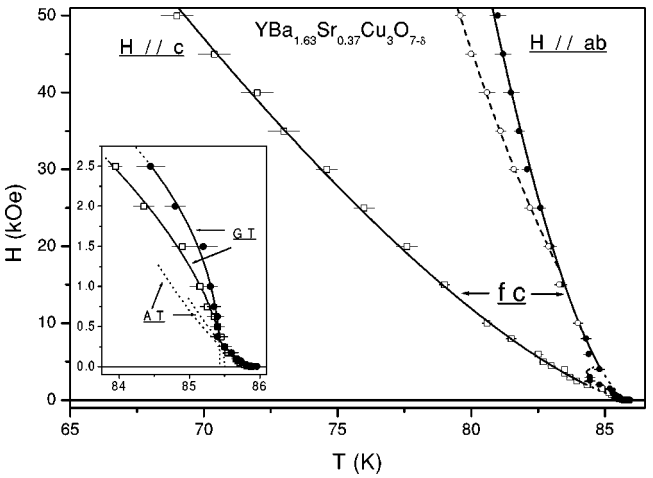


FIG. 9. Same as Fig. 6, but for a sample $YBa_{1.63}Sr_{0.37}Cu_3O_{7-\delta}$ single crystal, including measurements for $H\|ab$ wiht $H$ parallel to TP's or at 45° off the TP's.

the respective data for $H\|c$ from Ref. 33. In addition, Fig. 8 displays the $T_{irr}(H)$ data for $H\|c$ and $H\|ab$ of another $YBa_{1.75}Sr_{0.25}Cu_3O_{7-\delta}$ single crystal of the same batch as that of Fig. 6. Except for different $T_c$ values (see Fig. 1) and for somewhat different slopes, the overall aspect of the irreversibility profiles of all these samples are very similar.

Corrections for a demagnetizing field, although somewhat increasing the overall slope of the irreversibility line $T_{irr}(H)$ for $H\|c$, is very small for $H\|ab$. We have not corrected the data for demagnetizing fields, since they do not change the main trend of the $T_{irr}(H)$ lines and are innocuous to all our conclusions.

The most important features common to all samples are the strong $c$-axis/$ab$-plane anisotropies of $T_{irr}(H)$ in the high-field region and the characteristic marks of the Josephson flux dynamics in the low-field region of the doped single crystals; see the insets in Figs. 6, 7, and 8. In the major high-field region ($H>8$ kOe), where the flux dynamics is dominated by the Abrikosov vortices, the $T_{irr}(H)$ data for $H\|c$ could be well fitted in the whole field range by the fc power law. However, all attempts to fit the corresponding high-field $T_{irr}(H)$ data for $H\|ab$, in the whole field range, by a unique power law failed. This is because all these data exhibit a curious kink at about 30 kOe, suggesting two different regimes, one above and another below 30 kOe. In this lower-field range (8 kOe$<H<$30 kOe) the data could be well fitted by Eq. (1); see the fitting parameters in Table I. After seeing Ref. 25, where a similar kink was observed in a twinning monodomain melt-textured $YBa_2Cu_3O_{7-\delta}$ sample and explained in terms of the anisotropic pinning by TP's, we conjectured that the kinks in our $T_{irr}(H)$ data should have the same origin. Indeed, all the single crystals used in our irreversibility studies to this point show a mosaiclike twinning landscape, and we did not take care to align the TP's along the field.

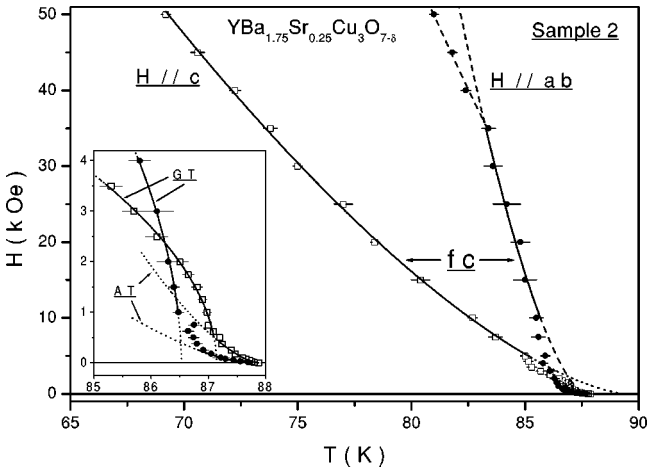


FIG. 8. Same as Fig. 6, but for another single crystal of the $YBa_{1.75}Sr_{0.25}Cu_3O_{7-\delta}$ (sample 2).

In order to make a closer investigation of the contribution of the TP's, we prepared a batch of $YBa_{1.63}Sr_{0.37}Cu_3O_{7-\delta}$ single crystals of intermediary Sr concentration. After selecting a single crystal, presenting a twinning configuration similar to the previously measured ones, we made a full sequence of measurements of $T_{irr}(H)$ for fields applied along the $c$ axis and along the $ab$ plane. For $H\|ab$ we remark that the irreversibility in the difference plots $\Delta M$ (see examples in Fig. 4) for fields parallel to the TP's starts at a higher temperature than for the same field applied 45° off of the TP's, but is considerably less abrupt. We understand this more gradual rise of the irreversibility as an indication that only a part of the magnetic flux is effectively pinned by the TP's. The whole set of $T_{irr}(H)$ data, shown in the $H$-$T$ diagram of Fig. 9, clearly reveals a contribution related to the orientation of the field with respect to the TP's above 30 kOe. While our $T_{irr}(H)$ data for $H\|ab$ and $H$ parallel to TP's could be well fitted by Eq. (1) in the whole field range above 8 kOe, the data for $H$ at 45° off of the TP's could be fitted by this power law only up to a maximum of 30 kOe, where these data coincide within experimental precision with those for $H$ parallel to TP's. All our fitting parameters are listed in Table I. The dashed line through the $T_{irr}(H)$ data above 30 kOe in Figs. 6–9 are guides to the eye.

In the low-field region (typically $H<8$ kOe) the $T_{irr}(H)$ data for all our granular superconducting samples, regardless

of fields applied along the $c$ axis or the $ab$ plane, are very similar, and systematically exhibit the symptoms of the Josephson flux dynamics in a frustrated superconductor. The continuous lines through the $T_{irr}(H)$ data in the insets of Figs. 6–9, indicated by AT and GT, are fittings to Eqs. (2) and (3), respectively (see the fitting parameters in Table I). These AT and GT features were also observed in previous magnetic irreversibility studies in polycrystalline as well as in single-crystal $YBa_{2-x}Sr_xCu_3O_{7-\delta}$ compounds for $H\|c$.[12,30–33] The AT and GT power laws are originally known from the magnetic irreversibility lines of spin glasses,[41] and are the fingerprints of frustrated systems. In this low-field region our $T_{irr}(H)$ data also exhibit a relatively small anisotropy for $H\|c$ or $H\|ab$. Curiously this anisotropy is systematically reversed with respect to that in high fields, and cannot be inverted by correcting for a demagnetizing field once these corrections would increase it a little bit. Another systematic and curious feature of the $T_{irr}(H)$ data for $H\|ab$ occurs near 8 kOe, where the Abrikosov flux dynamics takes over the dominance of the Josephson flux dynamics. There, a sudden increase of the flux pinning strength with increasing field is seen, an event analogous to the peak effect in hysteresis cycles. Apparently it signals the onset of the pinning by the TP's.

## IV. DISCUSSION

When the trapped flux is acted upon by a motive force lower than the critical strength, but sufficiently assisted by thermal activation, it creeps in the form of a damped motion of isolated fluxons. This dissipative motion is the origin of the irreversibility. An increasing applied magnetic field is well known to affect the effectiveness of the pinning mechanisms, chiefly that of the Josephson-junctions, which is especially sensitive to fields.[40] Therefore flux dynamics, particularly at the irreversibility limit, is expected to reflect much of the physics involved in the flux stabilizing mechanisms. This is especially the case in the low-field region of granular superconductors where the Josephson-flux dynamics is dominant and flux pinning by junctions and weak links is largely gauged by disorder and frustration. However, in order to obtain access to this physics it is essential to obtain precise and sufficiently detailed irreversibility data.

The density and precision of our measurements of $T_{irr}(H)$, allowed us to put into evidence finer details of the magnetic irreversibility line of our granular HTSC's. For instance, we could see the effect of the strongly anisotropic pinning of the TP's. But the most relevant features are those of the AT- and GT-like regimes, respectively [Eqs. (2) and (3)], that were previously found in several granular superconductors.[12,30–33] The fact that most irreversibility studies in the literature, which certainly did not all use nearly perfect single crystals, did not detect these details is due mainly to the excessive discreteness of the data points, especially in the low-field region. But another crucial point concerns the method used to extract the irreversibility limit from the raw data.

In reality the profiles of our data are not in isolation with those of other detailed irreversibility studies. For instance the general trend of the $T_{irr}(H)$ data of a $Bi_{2.2-x}Pb_xSr_{1.8}CaCu_2O_y$,[42] $Bi_{2.15}Sr_{1.85}CaCu_2O_{8+\delta}$,[43] and $Hg_{0.7}Pb_{0.3}Ba_2Ca_2Cu_3O_y$[44] superconductors show, in addition to the typical high-field flux-creep regime, two low-field regimes that recall quite well the $H-T$ diagrams of our doped single crystals. Recently the magnetic irreversibility data of a Sr-doped $YBa_2Cu_4O_8$ single crystal in fields up to 5 kOe,[45] applied along the $c$ axis, also indicated two regimes in this field region that are compatible with AT- and GT-like power laws.

The possible theoretical meaning of the AT- and GT-like power-law regimes of $T_{irr}(H)$ in granular superconductors was discussed, based on the completely analogous behaviors of the magnetic irreversibility of the spin glasses, in several previous papers.[12,33,46] The key ingredient giving rise to these power-law regimes is frustration. It arises from the disorder and the multiconnectedness of such superconducting grain aggregates.[40] It is important to remark that the superconducting granularity of the HTSC's is not just polycrystallinity. Due to the very short coherence length of the Ginsburg-Landau order parameter of these materials,[14] any lattice defects, extended or localized, give rise to a granular character even in the case of single crystals.[15,33] Moreover, a partial substitution of Ba by Sr, in polycrystalline $YBa_2Cu_3O_{7-\delta}$, has been verified to cause a decrease in the coherence length,[30] thereby sharpening the already steep topology of the GL order parameter even more. This, while strengthening the superconducting granularity, also reinforces the AT- and GT-like regimes.

Another central aspect of our experimental results concerns the anisotropic flux pinning mechanisms. The origin of the large anisotropy between the $T_{irr}(H)$ branches for $H\|c$ and $H\|ab$ in the high-field region is well known to be intrinsic to the planar superconducting structure of HTSC's. In low fields, where granularity effects and the Josephson flux dynamics are dominant, the anisotropy of the magnetic irreversibility could hardly be expected to be large. Effectively our $T_{irr}(H)$ data show only a very small anisotropy in this low-field range; curiously this is systematically the converse of that in high fields. This small anisotropy is mainly a consequence of the fact that the slope (see $H_0^{AT}$ values in Table I) in the AT-like range of $T_{irr}(H)$ is systematically lower for $H\|ab$ than for $H\|c$. But this reverses in the field range where GT-like regimes hold (see the $H_0^{GT}$ values in Table I). These facts suggest that in the AT-like regime the phase disorder induced by the field is more drastic when it points along the $ab$ plane. This is precisely what we expected, given that the weaker junctions along the $c$ axis come into question only for fields applied along the $ab$ planes. Nevertheless, for reasons that are not clear at this moment, the slopes of $T_{irr}(H)$ for $H\|ab$ and $H\|c$ in the range of the GT regime are reversed with respect to those in the AT range.

The newest feature of the $T_{irr}(H)$ data, disclosed in the present work, is a contribution of the anisotropic pinning of the TP's to the magnetic irreversibility for $H\|ab$. This anisotropic pinning, that depends on the field orientation with respect to the TP's, adds up to the planar anisotropy leading to Bose-glass or vortex-glass properties. The role of the TP's

becomes clear considering that the $CuO_2$ planes are [001]-like while the TP's are [110]- or $[1\bar{1}0]$-like. The intersections of the weaker superconducting layers, sandwiched between the $CuO_2$ planes, with TP's that can take two possible orthogonal directions, constitute correlated one-dimensional defects analogous to columnar defects. For $H\|ab$ and $H$ aligned with a family of TP's, the flux lines, already trapped between the $CuO_2$ planes by the intrinsic pinning, lock into the TP's to a considerable extent, resulting in a significant additional pinning energy. For $H>30$ kOe the flux line matter becomes very rigid. Therefore, if $H\|ab$ and the single crystal is rotated about the $c$ axis, the fluxons eventually are prevented from locking into the TP's if the angle of the field with respect to the TP's exceeds a critical value. This causes a loss of the additional pinning and a shift of the irreversibility limit to the lower-temperature side.[25] The variation of the flux pinning strength as a function of this angular displacement is cusplike. This critical directional behavior is usually seen as the distinctive behavior of a bosonlike system. In the case of HTSC's it is a Bose-glass phase, because the fluxon configuration is already glassy as a result of the random pinning defects. Nevertheless, for fields below 30 kOe, where the irreversibility temperature is high enough to cause large fluctuations of the flux lines and a softening of the vortex line lattice, the vortices are allowed to better accommodate them into the defects. However, within these conditions the flux pinning is isotropic, produced by the collectivity of the defects and dominated by the TP's. This enhances the magnetic irreversibility isotropically about the $c$ axis, so that in this field region only the vortex-glass features are met.

The fact that we could well fit our high-field $T_{irr}(H)$ data for $H\|ab$ and parallel to TP's by the fc power law from flux-creep theories in the whole field range indicates that these very anisotropic pinning effects, not considered in conventional flux creep theories, do not invalidate the general trends of this theoretical approach in high fields, at least in what concerns the magnetic irreversibility.

In summary, our results for the $T_{irr}(H)$ of granular HTSC's, besides confirming the intrinsic planar anisotropy, show that the conventional flux-creep regime is valid in a vast high-field region. Moreover, the cusplike variation of $T_{irr}(H)$ about the direction of the TP's for rotations of the single crystals about the $c$ axis in fields above 30 kOe and for $H\|ab$ attest to the properties of a Bose-flux-glass. Its more isotropic behavior for angles above a critical value or for any angle in field values below 30 kOe and above 8 kOe denotes vortex-glass features. On the other hand, the behavior of $T_{irr}(H)$, according to AT- and GT-like power laws in fields below 8 kOe, where the Josephson flux dynamics dominates, indicates a frustrated system.

## ACKNOWLEDGMENTS

The authors thank the Brazilian agencies CNPq and CAPES, and the PRONEX program for financial support.

*Corresponding author. Present address: Instituto de Física, UFRGS, Av. Bento Gonçalves, 9500, P.O. Box 15051, CEP 91501-970, Porto Alegre-RS, Brasil. FAX: (55) (51) 3316 7286. Email address: schaf@if.ufrgs.br

[1] Y. Yeshurun and A.P. Malozemoff, Phys. Rev. Lett. **60**, 2202 (1988).
[2] G. Blatter and B. Ivlev, Phys. Rev. Lett. **70**, 2621 (1993).
[3] A. Shilling, H.R. Ott, and Th. Wolf, Phys. Rev. B **46**, 14 253 (1992).
[4] G.T. Seidler, T.F. Rosenbaum, D.L. Heinz, J.W. Downey, A.P. Paulikas, and B.W. Veal, Physica C **183**, 333 (1991).
[5] N.E. Hussey, H. Takagi, N. Mori, N. Takeshita, Y. Iye, S. Adachi, and Tanabe, J. Supercond. **12**, 583 (1999).
[6] D.A. Cardwell, N. Hari Babu, W. Lo, and A.M. Campbell, Supercond. Sci. Technol. **13**, 646 (2000).
[7] J. Schaf, P. Rodrigues, Jr., P. Pureur, L. Ghivelder, Farun. Lu, E.L. Wolf, L.F. Cohen, L.R. Tessler, and K.N.R. Taylor, Physica C **235-240**, 2803 (1994).
[8] T. Higuchi, S.I. Yoo, and M. Murakami, Supercond. Sci. Technol. **11**, 138 (1998).
[9] Y.S. Song, M. Hirabayashi, H. Ihara, and M. Tokumoto, Phys. Rev. B **50**, 16 644 (1994).
[10] P.W. Anderson and Y.B. Kim, Rev. Mod. Phys. **36**, 39 (1964).
[11] P. Pureur, J. Schaf, and J.V. Kunzler, Prog. High Temp. Supercond. **9**, 137 (1988).
[12] P. Rodrigues, Jr., J. Schaf, and P. Pureur, Phys. Rev. B **49**, 15 292 (1994).
[13] J. Schaf, P. Pureur, and J.V. Kunzler, Phys. Rev. B . **40**, 6948 (1989).
[14] G. Deutscher and K.A. Muller, Phys. Rev. Lett. **59**, 1745 (1987).
[15] M. Daeumling, J.M. Seuntjens, and D.C. Larbalestier, Nature (London) **346**, 332 (1990).
[16] M.P.A. Fisher, Phys. Rev. Lett. **62**, 1415 (1989).
[17] J.D. Reger, T.A. Tokuyasu, A.P. Young, and M.P.A. Fisher, Phys. Rev. B **44**, 7147 (1991).
[18] J. Toner, Phys. Rev. Lett. **67**, 2537 (1991).
[19] D.A. Huse and H.S. Seung, Phys. Rev. B **42**, 1059 (1990).
[20] A.T. Dorsey, M. Huang, and M.P.A. Fisher, Phys. Rev. B **45**, 523 (1992).
[21] R.H. Koch, V. Foglietti, W.J. Gallagher, G. Koren, A. Gupta, and M.P.A. Fisher, Phys. Rev. Lett. **63**, 1511 (1989).
[22] L. Civale, A.D. Marwick, T.K. Worthington, M.A. Kirk, J.R. Thompson, L. Krusin-Elbaum, Y. Sun, J.R. Clem, and F. Holtzberg, Phys. Rev. Lett. **67**, 648 (1991).
[23] D. Bourgault, S. Bouffard, M. Toulemonde, D. Groult, J. Provost, F. Studer, N. Nguyen, and B. Raveau, Phys. Rev. B **39**, 6549 (1989).
[24] H. Safar, S.R. Foltyn, Q.X. Jia, and M.P. Maley, Philos. Mag. B **74**, 647 (1996).
[25] S. Sanfilippo, A. Sulpice, O. Laborde, D. Bourgault, Th. Fournier, and R. Tournier, Phys. Rev. B **58**, 15 189 (1998).
[26] W.K. Kwok, U. Welp, G.W. Crabtree, K.G. Vandervoort, R. Hulscher, and J.Z. Liu, Phys. Rev. Lett. **64**, 966 (1990).
[27] J.Z. Liu, Y.X. Jia, R.N. Shelton, and M.J. Fluss, Phys. Rev. Lett. **66**, 1354 (1991).
[28] D. Braithwaite, D. Bourgault, A. Sulpice, J.M. Barbut, R. Tournier, I. Monot, M. Lepropre, J. Provost, and G. Desgardin, J. Low Temp. Phys. **91**, 1 (1993).

[29] K. Saito, H.U. Nissen, and C. Beeli, Phys. Rev. B **58**, 6645 (1998).
[30] V.N. Vieira, P. Pureur, and J. Schaf, Physica C **353**, 241 (2001).
[31] V.N. Vieira, J. Schaf, and P. Pureur, Physica C **354**, 299 (2001).
[32] V.N. Vieira, J.P. da Silva, and J. Schaf, Physica C **341-348**, 1155 (2000).
[33] V.N. Vieira, J.P. da Silva, and J. Schaf, Phys. Rev. B **64**, 094516 (2001).
[34] J.R.L. de Almeida and D.J. Thouless, J. Phys. A **11**, 983 (1978).
[35] M. Gabay and G. Toulouse, Phys. Rev. Lett. **47**, 201 (1981).
[36] J. Golben and M. Vlasse, Supercond. Sci. Technol. **5**, 231 (1991).
[37] F. Licci, A. Gauzzi, M. Marezio, G.P. Radaelli, R. Masini, and C. Chaillout-Bougerol, Phys. Rev. B **58**, 15 208 (1998).
[38] M. Kakihana, S.G. Eriksson, L. Brjesson, L.G. Johansson, C. Strm, and M. Kll, Phys. Rev. B **47**, 5359 (1993).
[39] J.R. Rojas, R.M. da Costa, P. Pureur, and P. Prieto, Phys. Rev. B **61**, 12 457 (2000).
[40] W.Y. Shih, C. Ebner, and D. Stroud, Phys. Rev. B **30**, 114 (1984); **31**, 165 (1985).
[41] G.G. Kenning, D. Chu, and R. Orbach, Phys. Rev. Lett. **66**, 2923 (1991).
[42] Y. Nakayama, T. Motohashi, K. Otzschi, J. Shimoyama, K. Kitazawa, K. Kishio, M. Konczykowski, and N. Chikomoto, Phys. Rev. B **62**, 1452 (2000).
[43] D. Zech, S.L. Lee, H. Keller, G. Blatter, P.H. Kes, and T.W. Li, Phys. Rev. B **54**, 6129 (1996).
[44] Y. Zhuo, Su-Mi Oh, Jac-Hyuk Choi, Mun-Seog Kim, Sung-Ik Lee, N.P. Kiryakov, M.S. Kuznetzov, and S. Lee, Phys. Rev. B **60**, 13 094 (1999).
[45] M. Angst, S.M. Kazakov, J. Karpinski, A. Wisniewski, R. Puzniak, and M. Baran, Phys. Rev. B **65**, 094518 (2002).
[46] A.R. Jurelo, P. Pureur, and J. Schaf, Phys. Rev. B **64**, 174502 (2001).